The K-Segment of Maize DHN1 Mediates Binding to Anionic Phospholipid Vesicles and Concomitant Structural Changes[1][W][OA]

Myong-Chul Koag[2], Stephan Wilkens, Raymond D. Fenton, Josh Resnik, Evanly Vo, and Timothy J. Close*

Graduate Program in Biochemistry and Molecular Biology (M.-C.K., S.W., T.J.C.), Department of Botany and Plant Sciences (M.-C.K., R.D.F., J.R., E.V., T.J.C.), and Department of Biochemistry (S.W.), University of California, Riverside, California 92521–0124

Dehydrins (DHNs; late embryogenesis abundant D11 family) are a family of intrinsically unstructured plant proteins that accumulate in the late stages of seed development and in vegetative tissues subjected to water deficit, salinity, low temperature, or abscisic acid treatment. We demonstrated previously that maize (*Zea mays*) DHNs bind preferentially to anionic phospholipid vesicles; this binding is accompanied by an increase in α-helicity of the protein, and adoption of α-helicity can be induced by sodium dodecyl sulfate. All DHNs contain at least one "K-segment," a lysine-rich 15-amino acid consensus sequence. The K-segment is predicted to form a class A2 amphipathic α-helix, a structural element known to interact with membranes and proteins. Here, three K-segment deletion proteins of maize DHN1 were produced. Lipid vesicle-binding assays revealed that the K-segment is required for binding to anionic phospholipid vesicles, and adoption of α-helicity of the K-segment accounts for most of the conformational change of DHNs upon binding to anionic phospholipid vesicles or sodium dodecyl sulfate. The adoption of structure may help stabilize cellular components, including membranes, under stress conditions.

When plants encounter environmental stresses such as drought or low temperature, various responses take place to adapt to these conditions. Typical responses include increased expression of chaperones, signal transduction pathway and late embryogenesis abundant (LEA) proteins, osmotic adjustment, and induction of degradation and repair systems (Ingram and Bartels, 1996).

Dehydrins (DHNs; LEA D11 family) are a subfamily of group 2 LEA proteins that accumulate to high levels during late stages of seed development and in vegetative tissues subjected to water deficit, salinity, low temperature, or abscisic acid (ABA) treatment (Svensson et al., 2002). Some DHNs are expressed constitutively during normal growth (Nylander et al., 2001; Rorat et al., 2004, 2006; Rodriguez et al., 2005). DHNs exist in a wide range of photosynthetic organisms, including angiosperms, gymnosperms, algae, and mosses (Svensson et al., 2002). DHNs are encoded by a dispersed multigene family and are differentially regulated, at least in higher plants. For example, 13 *Dhn* genes have been identified in barley (*Hordeum vulgare*), dispersed over seven genetic map locations (Choi et al., 1999; Svensson et al., 2002) and regulated variably by drought, low temperature, and embryo development (Tommasini et al., 2008). DHNs are localized in various subcellular compartments, including cytosol (Roberts et al., 1993), nucleus (Houde et al., 1995), chloroplast (Artus et al., 1996), vacuole (Heyen et al., 2002), and proximal to the plasma membrane and protein bodies (Asghar et al., 1994; Egerton-Warburton et al., 1997; Puhakainen et al., 2004). Elevated expression of *Dhn* genes generally has been correlated with the acquisition of tolerance to abiotic stresses such as drought (Whitsitt et al., 1997), salt (Godoy et al., 1994; Jayaprakash et al., 1998), chilling (Ismail et al., 1999a), or freezing (Houde et al., 1995; Danyluk et al., 1998; Fowler et al., 2001). The differences in expression and tissue location suggest that individual members of the *Dhn* multigene family have somewhat distinct biological functions (Close, 1997; Zhu et al., 2000; Nylander et al., 2001). Many studies have observed a positive correlation between the accumulation of DHNs and tolerance to abiotic stresses (Svensson et al., 2002). However, overexpression of a single DHN protein has not, in general, been sufficient to confer stress tolerance (Puhakainen et al., 2004).

DHNs are subclassified by sequence motifs referred to as the K-segment (Lys-rich consensus sequence),

[1] This work was supported by the University of California (Biotechnology Research and Education grant no. 97–15), the National Science Foundation (grant no. IBN 92–05269), and the University of California Agricultural Experiment Station (Hatch grant no. 5306).

[2] Present address: Department of Physiology, University of California, Los Angeles, CA 90095.

* Corresponding author; e-mail timothy.close@ucr.edu.

The author responsible for distribution of materials integral to the findings presented in this article in accordance with the policy described in the Instructions for Authors (www.plantphysiol.org) is: Timothy J. Close (timothy.close@ucr.edu).

[W] The online version of this article contains Web-only data.

[OA] Open Access articles can be viewed online without a subscription.

www.plantphysiol.org/cgi/doi/10.1104/pp.109.136697

the Y-segment (N-terminal conserved sequence), the S-segment (a tract of Ser residues), and the ϕ-segment (Close, 1996). Because of high hydrophilicity, high content of Gly (>20%), and the lack of a defined three-dimensional structure in the pure form (Lisse et al., 1996), DHNs have been categorized as "intrinsically disordered/unstructured proteins" or "hydrophilins" (Wright and Dyson, 1999; Garay-Arroyo et al., 2000; Tompa, 2005; Kovacs et al., 2008). On the basis of compositional and biophysical properties and their link to abiotic stresses, several functions of DHNs have been proposed, including ion sequestration (Roberts et al., 1993), water retention (McCubbin et al., 1985), and stabilization of membranes or proteins (Close, 1996, 1997). Observations from in vitro experiments include DHN binding to lipid vesicles (Koag et al., 2003; Kovacs et al., 2008) or metals (Svensson et al., 2000; Heyen et al., 2002; Kruger et al., 2002; Alsheikh et al., 2003; Hara et al., 2005), protection of membrane lipid against peroxidation (Hara et al., 2003), retention of hydration or ion sequestration (Bokor et al., 2005; Tompa et al., 2006), and chaperone activity against the heat-induced inactivation and aggregation of various proteins (Kovacs et al., 2008).

Intrinsically disordered/unstructured proteins that lack a well-defined three-dimensional structure have recently been recognized to be prevalent in prokaryotes and eukaryotes (Oldfield et al., 2005). They fulfill important functions in signal transduction, gene expression, and binding to targets such as protein, RNA, ions, and membranes (Wright and Dyson, 1999; Tompa, 2002; Dyson and Wright, 2005). The disorder confers structural flexibility and malleability to adapt to changes in the protein environment, including water potential, pH, ionic strength, and temperature, and to undergo structural transition when complexed with ligands such as other proteins, DNA, RNA, or membranes (Prestrelski et al., 1993; Uversky, 2002). Structural changes from disorder to ordered functional structure also can be induced by the folding of a partner protein (Wright and Dyson, 1999; Tompa, 2002; Mouillon et al., 2008).

The idea that DHNs interact with membranes is consistent with many immunolocalization studies, which have shown that DHNs accumulate near the plasma membrane or membrane-rich areas surrounding lipid and protein bodies (Asghar et al., 1994; Egerton-Warburton et al., 1997; Danyluk et al., 1998; Puhakainen et al., 2004). The K-segment is predicted to form a class A2 amphipathic α-helix, in which hydrophilic and hydrophobic residues are arranged on opposite faces (Close, 1996). The amphipathic α-helix is a structural element known to interact with membranes and proteins (Epand et al., 1995). Also, in the presence of helical inducers such as SDS and trifluoroethanol (Dalal and Pio, 2006), DHNs take on α-helicity (Lisse et al., 1996; Ismail et al., 1999b). We previously examined the binding of DHN1 to liposomes and found that DHNs bind preferentially to anionic phospholipids and that this binding is accompanied by an increase in α-helicity of the protein (Koag et al., 2003). Similarly, a mitochondrial LEA protein, one of the group III LEA proteins, recently has been shown to interact with and protect membranes subjected to desiccation, coupled with the adoption of amphipathic α-helices (Tolleter et al., 2007).

Here, we explore the basis of DHN-vesicle interaction using K-segment deletion proteins. This study reveals that the K-segment is necessary and sufficient for binding to anionic phospholipid vesicles and that the adoption of α-helicity of DHN proteins can be attributed mainly to the K-segment.

RESULTS

Purification of Mutant Proteins

To determine whether the K-segment is necessary for binding to lipid vesicles, K-segment deletion proteins (Fig. 1) were produced in *Escherichia coli* and purified. At the initial purification step, the high solubility of DHN1 at high temperature was utilized to prepare DHN1-enriched extracts. No difference was observed in the solubility of wild-type DHN1, ΔK1, ΔK2, and ΔK3 upon exposure to 70°C. SDS-PAGE and western blotting were used to analyze fractions of each purification step for each protein using anti-K-segment polyclonal antibody (Close et al., 1993) or anti-RAB17 antiserum for the K-segment deletion proteins (Jensen et al., 1998). The ΔK1 protein was further purified by cation-exchange chromatography using a Mono S column and a gradient from 230 to 280 mM NaCl (Supplemental Fig. S2A). The ΔK2 protein was also purified using a Mono S column with a gradient from 320 to 410 mM NaCl, followed by hydrophobic interaction chromatography using a Phenyl Superose column and a gradient from 750 to 680 mM $(NH_4)_2SO_4$ (Supplemental Fig. S2B). The ΔK3 protein was fractionated using a Mono S column with a gradient from 220 to 290 mM NaCl, followed by hydrophobic interaction chromatography using a Phenyl Superose column and a gradient from 740 to 660 mM $(NH_4)_2SO_4$. To obtain pure ΔK3 protein, an additional step of chromatography was performed using a Mono Q column and a gradient from 230 to 400 mM NaCl in 20 mM triethylamine (TEA), pH 10.0 (Supplemental Fig. S2C).

Matrix-Assisted Laser Desorption Ionization Time of Flight Spectrometry and Amino Acid Analysis

The apparent molecular mass of each purified mutant protein in SDS-PAGE is higher than expected when compared with wild-type DHN1 (Fig. 2). This disparity is particularly evident with the ΔK2 and ΔK3 deletions, where the predicted molecular masses are 15 and 13 kD and the apparent molecular masses are 27 and 26 kD, respectively. Matrix-assisted laser desorption ionization time of flight (MALDI-TOF) mass spectrometry and amino acid composition anal-

```
                    10         20         30         40         50         60
                    |          |          |          |          |          |
WT DHN1     MEYGQQGQHG HGATGHVDQY GNPVGGVEHG TGGMRHGTGT GGMGQLGEHG GAGMGGGQFQ
ΔK1         MEYGQQGQHG HGATGHVDQY GNPVGGVEHG TGGMRHGTGT GGMGQLGEHG GAGMGGGQFQ
ΔK2         MEYGQQGQHG HGATGHVDQY GNPVGGVEHG TGGMRHGTGT GGMGQLGEHG GAGMGGGQFQ
ΔK3         MEYGQQGQHG HGATGHVDQY GNPVGGVEHG TGGMRHGTGT GGMGQLGEHG GAGMGGGQFQ

                                  ---------K1-----------
                    70         80         90         100        110        120
                    |          |          |          |          |          |
WT DHN1     PAREEHKTGG ILHRSGSSSS SSSEDDGMGG RRKKGIKEKI KEKLPGGHKD DQHATATTGG
ΔK1         PAREEHKTGG ILHRSGSSSS SSSEDDGIR- ---------- ------GHKD DQHATATTGG
ΔK2         PAREEHKTGG ILHRSGSSSS SSSEDDGMGG RRKKGIKEKI KEKLPGGHKD DQHATATTGG
ΔK3         PAREEHKTGG ILHRSGSSSS SSSEDDGIR- ---------- ------GHKD DQHATATTGG

                                    --------K2--------
                    130        140        150        160
                    |          |          |          |
WT DHN1     AYGQQGHTGS AYGQQGHTGG AYATGTEGTG EKKGIMDKIK EKLPGQH
ΔK1         AYGQQGHTGS AYGQQGHTGG AYATGTEGTG EKKGIMDKIK EKLPGQH
ΔK2         AYGQQGHTGS AYGQQGHTGG AYATGTEGTG -------------------
ΔK3         AYGQQGHTGS AYGQQGHTGG AYATGTEGTG -------------------
```

Figure 1. Comparison of amino acid sequences of wild-type DHN1 and deletion mutants. The primary amino acid sequences of wild-type (WT) DHN1 and each K-segment mutant are shown. There are two altered amino acids in the ΔK1 and ΔK3 proteins (italics). Hyphens indicate deleted positions.

ysis of each protein were used to confirm the identity of each purified protein. The molecular mass of each protein determined by MALDI-TOF spectrometry was very similar to the calculated value for each protein (Fig. 3; Supplemental Table S1). The measured amino acid composition of each purified mutant protein was nearly identical to the predicted amino acid composition of each mutant construct (Supplemental Table S2).

Lipid-Binding Activity of K-Segment Deletion Proteins

The lipid-binding activity of maize (*Zea mays*) DHN1 and the deletion proteins was assayed using gel-filtration chromatography and western blot of column fractions as described previously (Koag et al., 2003). Based upon our previous finding that DHN1 has a strong interaction with anionic liposomes, a 1:1 mixture of PA (phosphatidic acid; anionic):PC (phosphatidylcholine; neutral) large unilamellar vesicles (LUVs) and 100% PC LUVs were prepared using an extrusion method described previously (Hope et al., 1985), and the LUV suspensions were incubated with DHN1 proteins at a 15:1 mass ratio of phospholipid to protein for 3 h at 25°C, as described previously (Koag et al., 2003). The intensity of the immunoblot of ΔK1 by anti K-segment antibody was lower compared with normal DHN1, and detection of ΔK2 and ΔK3 protein was even less apparent than that of ΔK1 protein. Therefore, antiserum raised against whole DHN1 (RAB17) protein of maize was used. As expected, there was no binding of any of the four proteins to LUVs composed solely of the neutral phospholipid PC (Fig. 4A). In contrast, normal DHN1 and the ΔK1 and ΔK2 proteins bound LUVs containing the anionic phospholipid PA (fractions 8 and 9; Fig. 4B). The ΔK3 protein, which is missing both of the K-segments, eluted at a specific fraction volume (fraction 18) of free protein on the precalibrated Superose 6 gel-filtration column (Fig. 4B) and therefore appears not to bind to LUVs of any composition. Together, these results show that either K-segment in DHN1 is sufficient for LUV binding and that the binding of DHN1 to LUVs is dependent on the presence of at least one K-segment.

Secondary Structural Change of Liposome-Bound Proteins

Circular dichroism (CD) spectra were measured to analyze structural changes of each protein upon binding to vesicles. The CD spectrum of normal DHN1 purified from *E. coli* has a peak of negative ellipticity at 195 to 200 nm and weak ellipticity around 222 nm, indicative of a lack of secondary structure (Fig. 5A). The CD spectrum is essentially identical to that of DHN1 purified from maize seed (Koag et al., 2003).

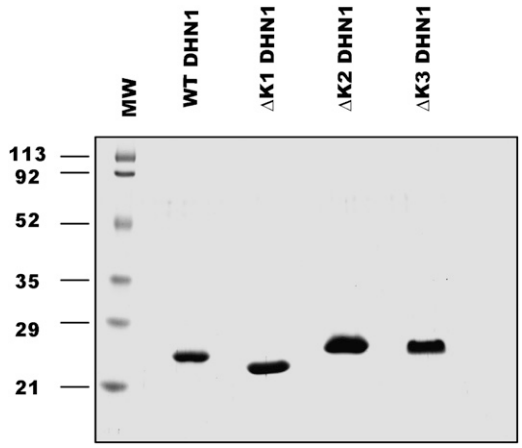

Figure 2. SDS-PAGE analysis of purified wild-type DHN1 and K-segment deletion proteins. The wild-type (WT) DHN1, ΔK1, ΔK2, and ΔK3 proteins were purified as described in the text. Each purified protein was analyzed by 13% SDS-PAGE. The masses of prestained molecular markers (MW) are designated in kilodaltons.

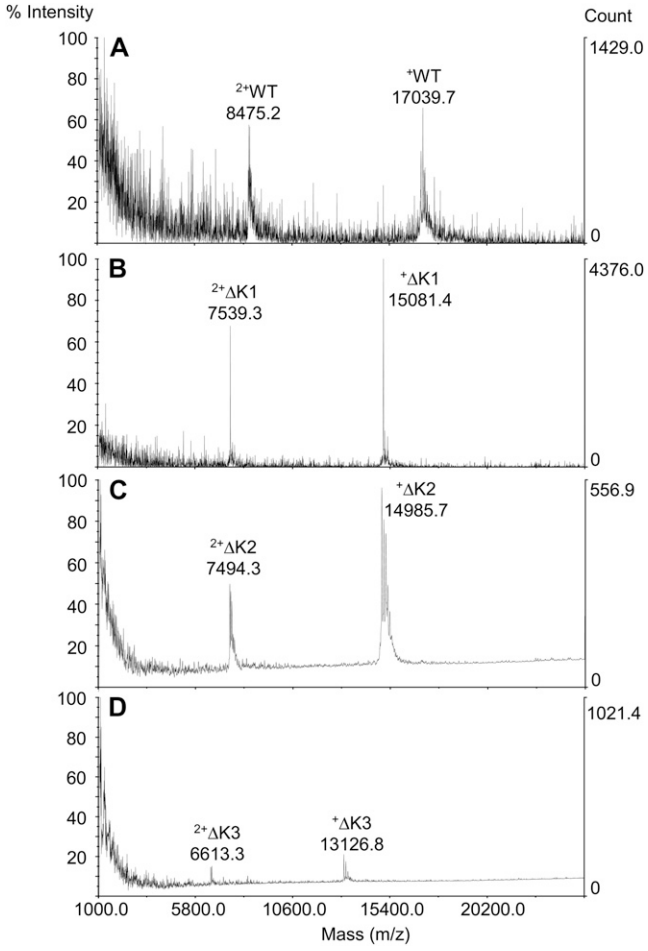

Figure 3. MALDI-TOF spectrometry of each DHN1 protein purified from *E. coli*. All mass spectra were acquired on a PerSeptive Biosystems Voyager DE-STR equipped with an N2 laser (337 nm, 3-ns pulse width, 3-Hz repetition rate). The mass spectra were acquired in the positive reflector mode with delayed extraction. The instrument's default mass calibration was used. The matrix used was sinapinic acid (10 mg mL^{-1}) in a 1:1 solution of acetonitrile and 0.1% trifluoroacetic acid. A, Wild-type (WT) DHN1. B, ΔK1 mutant. C, ΔK2 mutant. D, ΔK3 mutant.

Upon incubation with 100% PC vesicles, there was no significant change in the CD spectrum of DHN1 purified from *E. coli* (Fig. 5A). However, incubation of this DHN1 with 1:1 PA:PC vesicle ratio induced a significant transition of the spectrum at 190 to 230 nm (Fig. 5A). Particularly in the presence of either PC small unilamellar vesicles (SUVs) or PA SUVs, the pattern and intensity of CD spectra of DHN1 purified from *E. coli* are essentially identical to those previously reported for DHN1 from maize seed. These results indicate the adoption of partial α-helical conformation when DHN1 binds to vesicles containing PA. This established that the binding of DHN1 to anionic phospholipid-rich lipid vesicles is associated with a structural change in the protein (Fig. 5A), as previously reported for DHN1 derived from maize kernels (Koag et al., 2003).

The ΔK1 and ΔK2 deletion proteins, each of which contains only one K-segment, also displayed a shift in CD values upon incubation with 1:1 PA:PC SUVs but not with 100% PC SUVs (Fig. 5, B and C). The CD spectrum of both ΔK proteins changed significantly in the far-UV range (190–210 nm). The CD spectrum of ΔK2 also exhibited a shift in the 210- to 230-nm range in the presence of 1:1 PA:PC SUVs. These spectral shifts are consistent with the adoption of secondary structure by the K1 and K2 segments, and that some differences exist between the two.

The ΔK3 mutant, which is missing both K-segments, had no significant shift in the CD spectrum in the presence of 1:1 PA:PC SUVs or 100% PC SUVs (Fig. 5D). Therefore, similar to the lack of in vitro lipid vesicle binding described above, a conformational change seems also to depend on the K-segments. Analysis of the CD spectra of each DHN1 protein with anionic lipid vesicles using the structure analysis program CDSSTR and reference protein data set 7 showed that wild-type DHN1 adopts 5.0% α-helicity and the ΔK2 deletion protein adopts 4.2% α-helicity, while ΔK1 displays much less α-helical structure (Whitmore and Wallace, 2004). We note also that if the shifts in CD spectra of the ΔK1 and ΔK2 proteins with PA:PC SUVs are added together, then the sum very nearly reconstitutes the shift in the CD spectrum of normal DHN1 under the same conditions (Fig. 5E). This is consistent with the overall conformational change of DHN1 in association with anionic vesicles being attributed to a gain of structure of both K-segments.

Secondary Structure of DHN1 in the Presence of SDS

Wild-type DHN1 purified from maize seed underwent a structural transition not only upon binding to anionic phospholipid vesicles but also in the presence of SDS (Koag et al., 2003). Therefore, CD spectra were also measured in the presence of SDS to compare structural transitions with SDS with those from binding to vesicles. Analysis of the CD spectra using the CDSSTR program in Dichroweb (Whitmore and Wallace, 2004) indicates that wild-type DHN1 purified from *E. coli* gains 9.5% α-helical structure in the presence of 10 mM SDS (Fig. 6A). Compared with the transition in the CD spectrum induced by anionic phospholipids, the pattern in the presence of SDS is similar, although the amplitude of the transition around 220 nm is about double. The CD spectra of wild-type DHN1 purified from *E. coli* in the presence of 10 mM SDS and PA:PC SUVs are very similar to those of DHN1 purified from maize seed in their pattern and intensity (Koag et al., 2003).

The ΔK1 and ΔK2 deletion proteins, each of which contains only one K-segment, also underwent a shift in CD values upon incubation with 10 mM SDS (Fig. 6, B and C). The CD spectral changes of ΔK2 in the presence of 10 mM SDS (7.5% increase in α-helicity) were larger than those of ΔK1 (2% increase of

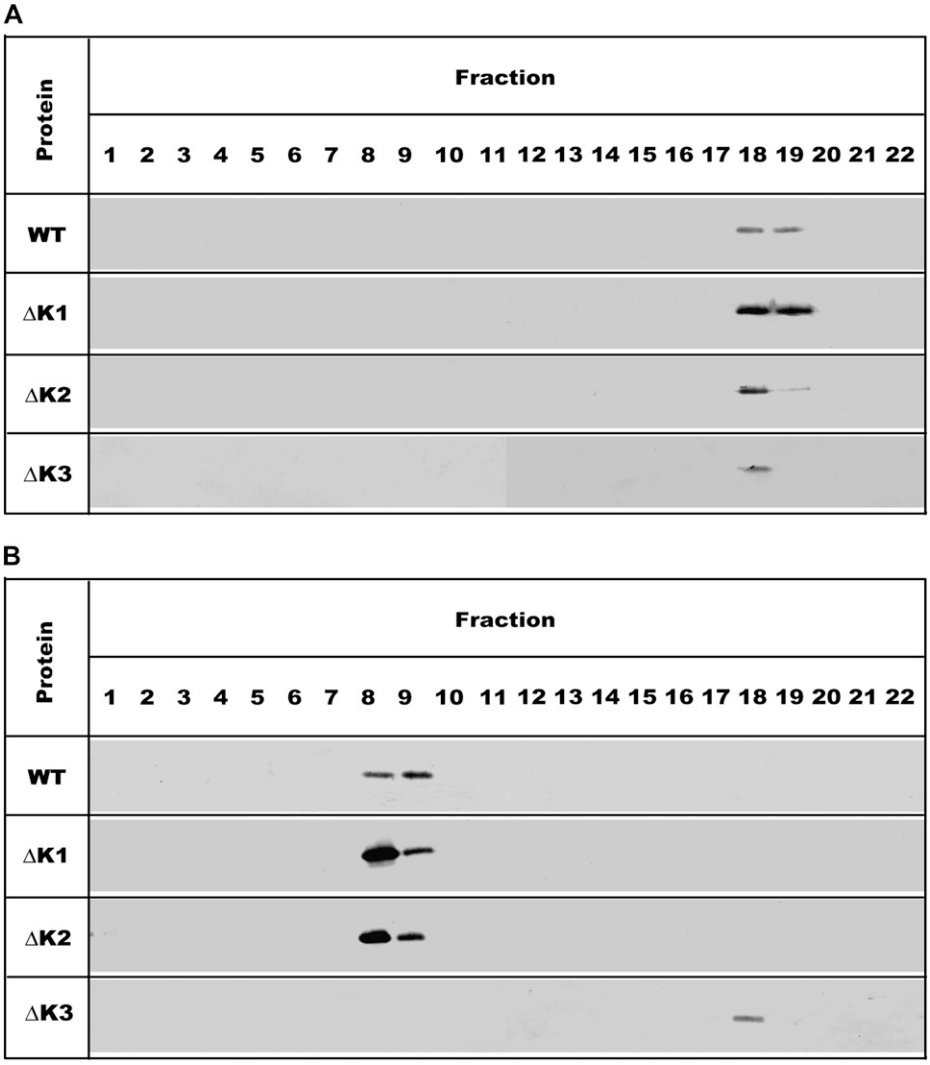

Figure 4. Western-blot analysis of gel-filtration fractions of each K-segment mutant with PC-LUVs or PA:PC-LUVs. Each mutant protein was incubated with LUVs at a 1:15 mass ratio of protein to phospholipid for 3 h at room temperature. The incubation mixture was separated over a calibrated Superose 6 gel column to determine whether the protein coelutes with liposomes. Each fraction was assessed by western blotting. The LUVs were in fractions 8 and 9, while free mutants proteins were in fractions 18 and 19. A, LUVs prepared from PC. B, LUVs prepared from a 1:1 mixture of PA and PC. WT, Wild type.

α-helicity). These spectral shifts indicate the adoption of secondary structure by the K1 and K2 segments, with some differences and additivity between the two.

The ΔK3 mutant, which is missing both K-segments, showed only a minor shift in the CD spectrum and no significant increase of α-helical structure in the presence of 10 mM SDS (Fig. 6D). If the shifts in CD spectra of the ΔK1 and ΔK2 proteins with SDS are added together, then the sum is nearly equal to the shift in the CD spectrum of normal DHN1 under the same conditions (Fig. 6E).

When the structural changes of each protein in the presence of 10 mM SDS were compared with those upon liposome binding, even though there are some differences such as intensity in the ellipticity around 220 nm, the effect of anionic phospholipid and SDS on the structural changes of DHN1 looks similar.

These observations are consistent with the idea that the overall conformational change of DHN1 in association with anionic vesicles and SDS is largely attributed to a gain of structure of both K-segments.

Secondary Structure of Synthetic K-Segment Peptide in the Presence of SDS and Liposomes

Because the CD data from each protein in the presence of anionic lipid vesicles and SDS imply that the structural changes of DHN1 protein are due to an interaction of K-segment with lipid vesicles or SDS, we also examined the CD spectra measurement of the synthetic K-segment peptide in the presence of SDS and liposomes. No structural transition was induced when the K-segment was incubated with 100% PC SUVs (Fig. 7). However, when the K-segment was incubated with either PA:PC liposomes or 10 mM SDS, a prominent induction of α-helix was observed. Similar to the wild-type and mutant DHN1 proteins, SDS causes a more substantial structural change of the K-segment than do vesicles containing anionic phos-

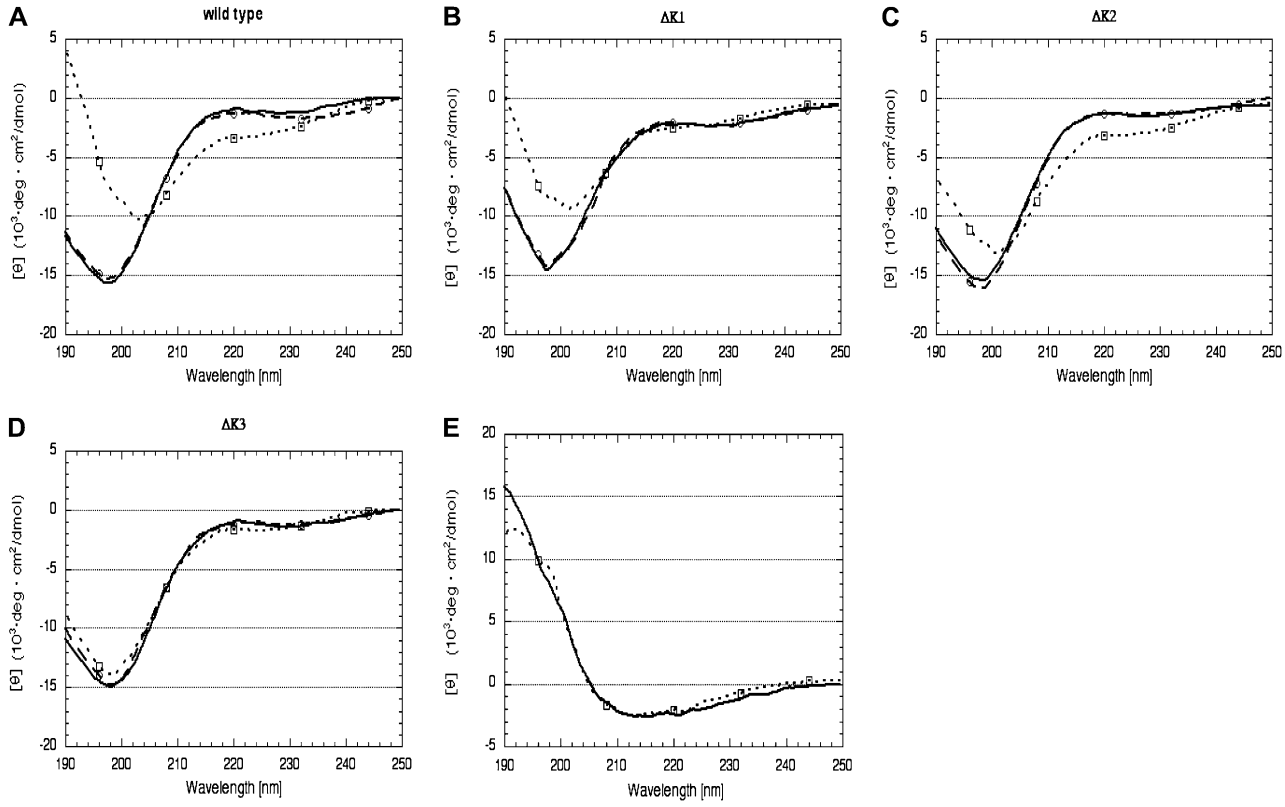

Figure 5. Transition in secondary structure of wild-type DHN1 and K-segment deletion mutants upon incubation with PC-SUVs or PA:PC-SUVs. The CD spectra of each protein in free form or in the presence of SUVs were measured. Spectra were corrected against buffer and liposome. Path length was 0.1 cm, step resolution was 0.5 nm, sensitivity was 100 millidegrees, accumulation was 8, scan speed was 50 nm min^{-1}, and bandwidth was 1.0 mm. Protein alone (solid lines), protein with PC-SUVs (circles, dashed lines), and protein with PA:PC-SUVs (squares, dotted lines) are shown. A, Wild-type DHN1. B, ΔK1 protein. C, ΔK2 protein. D, ΔK3 protein. E, Comparison of conformational transition upon binding to PA-SUVs between wild-type DHN1 and the sum of ΔK1 (B) and ΔK2 (C).

pholipids. Analysis of spectra of the K-segment using the CDSSTR program (Whitmore and Wallace, 2004) showed 22% α-helical structure at 10 mM SDS and 15% α-helical structure with the incubation of PA:PC liposomes. In general, these observations on the K-segment are also consistent with the idea that the K-segment undergoes a structural transition upon interaction with SDS or anionic vesicles, and this accounts for most of the structural transition that has been observed with the intact DHN1 protein under the same conditions.

DISCUSSION

To assess the structural and functional roles of the highly conserved K-segment of DHNs, a deletion mutation approach was used. Three K-segment deletion mutants (ΔK1, ΔK2, and ΔK3) were produced from maize DHN1 using site-directed mutagenesis and expression in *E. coli*. As a result of these deletions, the mutant proteins are more acidic than the wild-type protein (Supplemental Table S1). Mutant proteins were purified by a combination of ion-exchange and hydrophobic interaction chromatography (Supplemental Fig. S2, A–C). Each fraction containing the protein in each purification step was examined by SDS-PAGE and western blotting as described in "Materials and Methods." The identity of each mutant protein was confirmed by MALDI-TOF spectrometry and amino acid composition analysis (Fig. 3; Supplemental Tables S1 and S2). MALDI-TOF spectrometry of each protein gave molecular weights within 0.05% to 0.1% of predicted values, which is well within an acceptable range of accuracy (Hillenkamp et al., 1991). Three satellite peaks from the ΔK2 mutant have additional mass of 98 D each. This may be explained by the formation of H_2SO_4 adducts (+98 D) during the Phenyl Superose chromatographic step of purification. The intensity and numbers of SO_4 adducts can be increased by the amount of $(NH_4)_2SO_4$ used for the elution step (Prinz et al., 1999). The low peak intensity of the ΔK3 mutant may be explained by inefficient ion formation resulting from deletion of the highly charged K-segments.

The properties of high-temperature solubility, slow mobility in SDS-PAGE, and high solubility in 50%

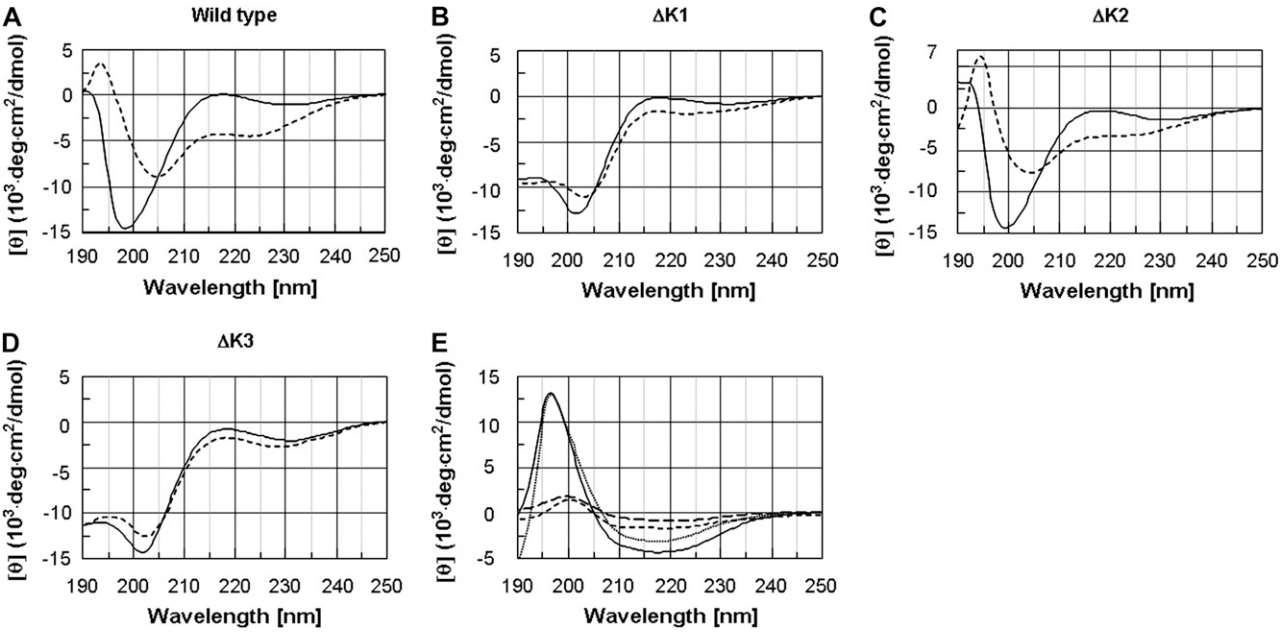

Figure 6. Transition in secondary structure of wild-type DHN1 and K-segment deletion mutants in the presence of SDS. The CD spectra of each protein in free form or in the presence of 10 mM SDS were measured. Spectra were corrected against buffer and 10 mM SDS. Path length was 0.1 cm, step resolution was 0.5 nm, sensitivity was 100 millidegrees, accumulation was 8, scan speed was 50 nm min^{-1}, and bandwidth was 1.0 mm. Protein alone (solid lines) and protein with 10 mM SDS (dashed lines) are shown. A, Wild-type maize DHN1 purified from *E. coli*. B, ΔK1 protein. C, ΔK2 protein. D, ΔK3 protein. E, Difference spectra (spectrum with 10 mM SDS minus spectrum with no SDS) for wild-type DHN1 (solid line), ΔK1 protein (short-dashed line), ΔK2 protein (dotted line), and ΔK3 protein (long-dashed line).

$(NH_4)_2SO_4$ are characteristic of the mutant proteins, much like wild-type DHN1. However, migration of the ΔK2 and ΔK3 deletion proteins in SDS-PAGE is even slower than for wild-type DHN1. This could be due to lower charge-charge association of the mutant proteins with SDS, resulting in less electrostatic pulling force, or retention of a less flexible structure that retards migration relative to wild-type DHN1 due to greater impedance with the polyacrylamide matrix.

It has been presumed that the K-segment is an essential unit relevant to the function of DHNs in response to dehydration-affiliated stresses (Close, 1996; Svensson et al., 2002) and that the K-segment can form an amphipathic α-helix, a biochemically important element involved in protein-protein and protein-lipid interactions (Dure, 1993; Epand et al., 1995). In our previous studies with wild-type maize DHN1 purified from the maize seed, we demonstrated that this protein binds to anionic phospholipid-rich vesicles and that this binding is accompanied by a gain of structure of the protein (Koag et al., 2003). In the lipid-binding assay with the K-segment deletion mutant proteins, the binding was still observed for the ΔK1 and ΔK2 single deletion mutants, while it was abolished for the ΔK3 double deletion mutant. These results indicate that the K-segment is necessary and sufficient for the binding of DHNs to anionic phospholipid vesicles (Fig. 4). The binding of nonphosphorylated forms of the protein is consistent with previous results from another research group (Kovacs et al., 2008).

As shown in Figure 5, the induction from unstructured to partially α-helical structure upon incubation with PA-containing anionic phospholipid vesicles is consistent with the binding of wild-type DHN1, ΔK1,

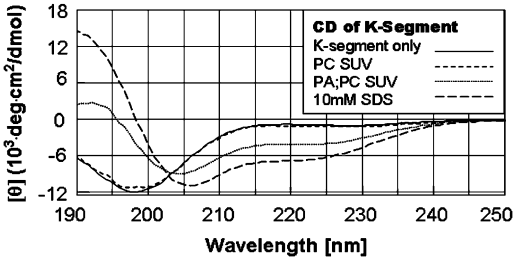

Figure 7. The effects of PA, PC, and SDS on the secondary structure of K-segment peptides. The CD spectra of synthetic K-segment peptides were measured in free form or in the presence of 10 mM SDS, PC liposome, and PA liposome. The concentration of the K-segment was adjusted to 20 μg mL^{-1} for every measurement. The K-segment was incubated with either PC or PA:PC liposomes at a 1:15 mass ratio of K-segment to phospholipid. The spectra were corrected against buffer, PC-SUVs, PA:PC-SUVs, and 10 mM SDS. Path length was 0.1 cm, step resolution was 0.5 nm, sensitivity was 100 millidegrees, accumulation was 9, scan speed was 50 nm min^{-1}, and bandwidth was 1.0 mm. K-segment alone (solid line), K-segment in the presence of PC-SUVs (short-dashed line), K-segment in the presence of PA:PC-SUVs (dotted line), and K-segment in the presence of 10 mM SDS (long-dashed line) are shown.

and ΔK2 proteins to LUVs. In contrast, there was no detectable transition in the CD spectrum of the ΔK3 double deletion protein with PA-containing vesicles, indicating that the change in structure detected by CD was dependent on the K-segments. Interestingly, when the changes in CD spectra of the ΔK1 and ΔK2 proteins upon incubation of PA SUVs are combined, the combination reconstitutes the change in the CD spectra of wild-type DHN by PA SUVs (Fig. 5E). So it seems that the K-segments of DHN1 may have a cumulative effect on the overall structure of the protein and that the structural change of DHNs due to an association with anionic phospholipids may be derived from conformational changes in K-segments. Additionally, as described in "Results," the CD spectrum of maize DHN1 prepared from maize seeds in a phosphorylated state (Koag et al., 2003) is nearly identical to the CD spectrum of maize DHN1 prepared from *E. coli* in a nonphosphorylated state. This is in good agreement with two recent reports that phosphorylation has no or only a marginal effect on structural changes in vitro (Mouillon et al., 2008) and on membrane binding (Kovacs et al., 2008). However, a recent study on the phosphoproteome showed evidence for mediation of phosphorylation effects through (1) conformational change coupled to phosphorylation, and (2) modulation of charge-charge interaction between protein and other cellular targets (Kitchen et al., 2008). Therefore, although phosphorylation does not lead to conformational changes in DHNs detectable in this study, it should not be ruled out that phosphorylation may affect lipid binding or can have some other functional role. In fact, prior studies of DHNs have shown that phosphorylation regulates nuclear localization (Jensen et al., 1998) and the binding of calcium ions (Heyen et al., 2002; Alsheikh et al., 2003; Brini et al., 2006).

Taken together, even though physicochemical conditions in plant cells under dehydrative stresses are very different from those typically used to characterize biochemical properties in vitro, the results of this study suggest that the K-segments of DHN1 may be responsible for binding to negatively charged membranes in vivo and that such binding is causally related to the adoption of structure of DHN1. It then follows also that the membrane-bound, structured form of DHN1 is a relevant element of the response of plant cells to environmental stresses that typically evoke DHN1 production.

While some LEA proteins (generally groups 3 and 4) adopt predominantly α-helical structure upon drying or addition of SDS or trifluoroethanol (Goyal et al., 2003; Shih et al., 2004; Tolleter et al., 2007), others (generally groups 1 and 2) assume only partial (about 10%) α-helical structure upon addition of trifluoroethanol, SDS, liposomes, and other helical inducers (Koag et al., 2003; Soulages et al., 2003; Shih et al., 2004; Mouillon et al., 2006, 2008). In accordance with those previous results, CD spectra of full-length DHN1 displayed low overall percentages of α-helical structure with SDS and liposomes, while a more prominent percentage of α-helical transition was observed with the K-segment alone. So, in line with one recent report (Mouillon et al., 2008), we refine the view of group 2 LEAs by clarifying that the structural change of full-length DHN can be attributed significantly to the conserved K-segment, which can adopt sufficient structure to account for most of the α-helicity of the entire DHN1 protein (Fig. 7). To confirm the structural changes of DHN1 bound to SDS and anionic phospholipid vesicles, multidimensional NMR spectra including ^{1}H-^{15}N heteronuclear single quantum coherence, known as a "fingerprint spectrum" of proteins, of DHN1 alone and of DHN1 in the presence of SDS, have been acquired (Koag, 2002). In the presence of SDS, nearly all of the cross-peaks for the K-segment of DHN1 in ^{1}H-^{15}N heteronuclear single quantum coherence disappeared or shifted. Compared with the spectrum of DHN1 alone, the positions of DHN1 cross-peaks that do not belong to the K-segment remained unchanged after binding to SDS, indicating that these cross-peaks represent amino acids that do not bind to anionic membrane vesicles or SDS and remain unfolded and mobile in the presence of them.

The plasma membrane of plants is known to be a major site of physical strain and damage under dehydrative stresses such as freezing and drought (Steponkus et al., 1998). It has been suggested that LEA proteins can contribute to membrane stabilization against those stresses (Artus et al., 1996; Danyluk et al., 1998; Koag et al., 2003; Tolleter et al., 2007; Kovacs et al., 2008). Recently, it has been shown that PA, which acts as a second messenger in stress signaling pathways (osmotic and oxidative stress, ABA treatment, wounding, and pathogen attack), accumulates over several hours of stress (Frank et al., 2000; Katagiri et al., 2005). PA-enriched membranes are induced to form a hexagonal phase II membrane structure under acidic pH conditions or with elevated concentrations of Ca^{2+} (Cullis et al., 1986). By binding to membranes through the K-segment amphipathic α-helix, DHNs may stabilize PA-enriched membranes such that they are less prone to transition into hexagonal phase II structures under stress conditions.

The role of DHN1 stabilization of membranes may be quite general given that all membrane-trafficking processes, such as transport between endoplasmic reticulum and Golgi, and galactolipid transport from the inner chloroplast envelope to the thylakoid, are mediated by vesicle formation. These processes require the hydrolysis of ATP or GTP, they require acetyl-CoA and vesicle-inducing proteins, and they show temperature dependence. Particularly in the transport of lipid to the thylakoid in chloroplasts of plants adapted to low temperature, vesicles accumulate in the stroma. It has been proposed that vesicle fusion is blocked at low temperature (Andersson et al., 2001). In addition, vesicles involved in membrane trafficking of the plasma membrane are very rich in

anionic phospholipids such as PA and phosphatidylserine (Liscovitch and Cantley, 1995).

A mitochondrial LEA protein was shown to interact with and protect membranes upon drying, with structural transition into amphipathic α-helices. The authors (Tolleter et al., 2007) observed no structural transition when the protein was exposed to lipid membranes in aqueous media; however, this is not contrary to our observations and might be expected, since the membranes were composed of neutral phospholipids, not anionic phospholipids, which for DHN1 at least are essential to membrane binding. There are indeed many examples of interactions between amphipathic α-helices and membranes that are sensitive to polarity and charges at the membrane interface and to the distribution of charged amino acid residues on helical peptides (Mishra and Palgunachari, 1996; White et al., 2001). At low water potential, columbic interaction increases due to a diminished effect of the dielectric constant of water. While the interaction between DHNs and membranes may require anionic phospholipids in a mainly aqueous environment, LEA proteins might interact also with neutral phospholipid membranes under conditions of lower water potential. This would be consistent with the observations involving the mitochondrial LEA protein.

DHNs bind to a range of metal ions with multiple tandem His residues (Svensson et al., 2000; Kruger et al., 2002) and can bind a large number of solute ions (Tompa et al., 2006). For example, the *Citrus unshiu* CuCOR19 DHN protein binds Cu^{2+} ions and scavenges reactive oxygen species, presumably to protect membranes from oxidative damage caused by water deficit (Hara et al., 2003, 2005). Members of the acidic subgroup of DHNs (ERD14, ERD10, and COR47) were observed to increase Ca^{2+} binding when phosphorylated in the poly-Ser motif (Alsheikh et al., 2003). It was also recognized that acidic residues of DHNs are involved in ion binding (Alsheikh et al., 2005). Water deficit can trigger an increase in metal ion concentration, which may cause stress to the plant directly and indirectly. An acidic DHN was observed to interact with membranes under cold stress (Danyluk et al., 1998). Recently, the nonphosphorylated forms of two acidic DHNs (ERD10 and ERD14) were reported to bind membranes through a peripheral electrostatic interaction with phospholipid head groups (Kovacs et al., 2008). More extensive studies on lipid- and metal-binding activities clearly are needed to determine whether the two affinities work synergistically.

In summary, our results support the hypothesis that the K-segments of DHNs constitute the interface through which DHNs bind the surface of membranes enriched in anionic phospholipids and that, upon such binding, the K-segments adopt an α-helical conformation whereas most of the remainder of the protein remains unstructured. More extensive studies on the binding partners of DHNs and structural aspects of the disordered-to-structured transition will help refine our understanding of the role of these proteins under environmental stresses.

MATERIALS AND METHODS

Construction of K-Segment Deletion Proteins

Deletion mutant forms of maize (*Zea mays*) DHN1 were constructed by introducing deletions of either or both K-segments. Oligonucleotide-directed mutagenesis was carried out following the manufacturer's protocol for the GeneEditor In Vitro Site-Directed Mutagenesis System (Promega) as follows. The pET19b-*Dhn1* (maize; Jepson and Close, 1995) plasmid was used as the starting material. Primers containing *Sac*II and *Nhe*I restriction sites were designed and used as mutagenic oligonucleotides (Supplemental Fig. S1). Denatured pET19b-*Dhn1* DNA was annealed to phosphorylated mutagenic oligonucleotides along with another oligonucleotide to modify the ampicillin resistance gene to confer resistance to Selection Antibiotic Mix. The mutant DNA strand was synthesized using T4 DNA polymerase and T4 DNA ligase. The reaction mixture was used to transform competent cells of *Escherichia coli* strain BMH71-18 *mut*S (repair defective) to establish a culture containing the desired mutant plasmid. Transformants were grown as a mixed culture in Luria-Bertani (LB) medium supplemented with 20 μg mL^{-1} Selection Antibiotic Mix. Strain DH5α was then transformed with plasmid DNA isolated from the BMH71-18 *mut*S mixed culture, and colonies were selected on LB agar containing 50 μg mL^{-1} ampicillin and 20 μg mL^{-1} Selection Antibiotic Mix. This second round of transformation separated wild-type from mutant plasmids. Several individual colonies were then analyzed by restriction enzyme digestion of plasmid DNA and sequencing with a T7 primer.

To generate a mutant missing the first K-segment (ΔK1), a pair of primers including a *Sac*II restriction site (underlined in 5′-GACGACGGCATCCGCGGAAGGAGGAAG-3′ and 5′-GGAGAAGCTGCCCCGCGGGCCACAAGGACG-3′) was used (Supplemental Fig. S1). For a mutant missing the second K-segment (ΔK2), a set of primers containing a *Nhe*I restriction site (underlined in 5′-GAGGGCACCGGCTAGCAGAAAGGCATTATC-3′ and 5′-GAGAAGCTGCCCGGCTAGCACTGAGCGCCC-3′) was used (Supplemental Fig. S1). For a double mutant lacking both K-segments (ΔK3), both primer pairs were used simultaneously (Supplemental Fig. S1). For the ΔK1 mutant, two of four selected colonies (MK102 and MK104) selected from the second-round transformation for site-directed mutagenesis were confirmed to contain the desired *Sac*II restriction enzyme sites. MK102 was chosen to digest with *Sac*II restriction enzyme and ligated with T4 ligase. Then the ligated construct was used to transform the *E. coli* DH5α competent cells. Three selected clones (MK1-1, MK1-2, and MK1-3) were verified to have the correct sequence. For the expression of ΔK1, construct MK1-2 was used. For the ΔK2 mutant, three colonies (MK201, MK202, and MK203) selected from the second-round transformation for site-directed mutagenesis were verified to include the *Nhe*I restriction site. MK202 was chosen to digest with the *Nhe*I restriction enzyme and ligated with T4 ligase. Then, the ligated construct was used to transform the *E. coli* DH5α competent cells. Three selected clones (MK2-1, MK2-2, and MK2-3) were verified to have the correct sequence. For the expression of ΔK2, construct MK2-2 was used.

For the ΔK3 mutant, two of five clones (MK301 and MK304) were proven to contain both the *Sac*II and *Nhe*I restriction sites by sequencing. MK301 was digested with *Sac*II and ligated with T4 ligase. Then the ligation reaction was used for transformation of *E. coli* DH5α competent cells to identify a ΔK1 deletion. Four selected colonies (MK31-1, MK31-2, MK31-3, and MK31-4) contained the correct sequence. Subsequently, MK31-4 was digested by *Nhe*I and religated. The religated construct was used for transformation of strain DH5α to screen for a double deletion mutant. Two of the chosen colonies (MK32-1 and MK32-2) were confirmed to possess the correct sequence. The construct MK32-2 was used for expression of ΔK2.

Two amino acids of ΔK1 and ΔK3 at positions 88 and 89 were changed from Met/Gly to Ile/Arg as a consequence of the site-directed mutagenesis shown in Figure 1. In addition, the molecular mass and pI values of each protein were altered as shown in Supplemental Table S1.

Protein Expression in *Escherichia coli*

BL21-CodonPlus (DE3)-RIL competent cells (Stratagene) were transformed with mutant constructs MK1-2, MK2-2, and MK32-2 according to the manufacturer's protocol. The transformation mixture was grown on LB agar plates

(100 μg mL^{-1} ampicillin and 20 μg mL^{-1} chloramphenicol) to select for transformants. LB medium containing 100 μg mL ampicillin^{-1} and 20 μg mL^{-1} chloramphenicol was inoculated with a fresh overnight culture of the *E. coli* expression strain with each DHN protein and grown to a cell density of 0.5 optical density at 600 nm. Isopropyl β-D-1-thiogalactopyranoside was added to a concentration of 1 mM to induce protein expression, and the culture was grown at 250 rpm and 37°C for an additional 2 h to a cell density of 1.0 optical density at 600 nm. Cells were harvested by centrifugation at 6,000*g* for 15 min at 4°C (Beckman J2-21, JS7.5 rotor). Cell pellets were stored at −80°C.

Purification of Deletion Mutant Proteins

Cell pellets were thawed on ice and resuspended in ice-cold lysis buffer (25 mM MES, pH 6.0, 20 mM NaCl, and 1 mM phenylmethylsulfonyl fluoride). Cells were lysed by passing twice through a French pressure cell (Thermo Fisher Scientific) with an internal pressure of 25,000 p.s.i. Cell debris was pelleted by centrifugation at 100,000*g* for 40 min at 4°C in a Beckman L8-M ultra centrifuge (Beckman Coulter) and 60 Ti rotor. The supernatant was heated to 70°C in a boiling-water bath for 10 min, cooled on ice, and centrifuged at 100,000*g* for 40 min at 4°C on a Beckman L8-M, 60 Ti rotor (Beckman Coulter) to pellet heat-insoluble proteins. The supernatant was diluted 1:1 in 25 mM MES, pH 6.0, filtered through a 0.2-μm pore size cellulose acetate membrane (GE Osmonics), and loaded onto a 5-mL HiTrap SP-HP column (GE Healthcare Amersham Biosciences) equilibrated with 25 mM MES, pH 6.0, and 20 mM NaCl. Proteins were eluted with a 96-mL 20 to 412 mM NaCl gradient in 25 mM MES, pH 6.0. Peak fractions were identified by SDS-PAGE and immunoblot. Pooled fractions from cation exchange were diluted 1:1 with 50 mM sodium phosphate, pH 7.0, and 100% saturated $(NH_4)_2SO_4$, pH 7.4, and incubated at 0°C for 1 h to precipitate proteins. The solution was centrifuge at 13,800*g* for 30 min at 4°C. The pellet was dissolved in 50 mM sodium phosphate, pH 7.0, and 1.4 M $(NH_4)_2SO_4$, pH 7.0, filtered through a 0.2-μm pore size cellulose acetate membrane (GE Osmonics), and loaded on a Phenyl Superose HR 10/10 column (GE Healthcare Amersham Biosciences) equilibrated in 50 mM sodium phosphate, pH 7.0, and 1.4 M $(NH_4)_2SO_4$, pH 7.0. Proteins were eluted with 120 mL of a 1.4 to 0 M $(NH_4)_2SO_4$ gradient in 50 mM sodium phosphate, pH 7.0. Peak fractions were identified by SDS-PAGE and pooled. Pure DHN was desalted with PD-10 desalting column (GE Healthcare Amersham Biosciences) according to the manufacturer's instructions and eluted in Milli-Q water (Millipore). Samples were dried in a SpeedVac concentrator (Thermo Scientific) and dissolved in Milli-Q water.

Anion Exchange

For the ΔK3 mutant protein, an additional purification step was applied. Pooled fractions from hydrophobic interaction chromatography were dialyzed against 20 mM TEA, pH 10.0. The dialysate was loaded on a Mono Q column (GE Healthcare Amersham Biosciences) equilibrated in 20 mM TEA, pH 10.0, and eluted with a 0 to 2 M NaCl gradient in 20 mM TEA, pH 10.0. Peak fractions were collected and examined by 13% SDS-PAGE and immunoblotting.

Immunoblotting

Immunoblotting was used for analysis of fractions at each purification step and for the lipid-binding assay. For wild-type DHN1, polyclonal antibody against the conserved K-segment was used as described previously (Close et al., 1993). To detect K-segment deletion proteins, anti-RAB17 antiserum (a gift from M. Pages) was used at a 1:500 dilution (Jensen et al., 1998).

MALDI-TOF Spectrometry

Mass spectra of normal and deletion mutant proteins were determined by MALDI-TOF on a Voyager DE-STR (PerSeptive Biosystems) equipped with an N2 laser (337 nm, 3-ns pulse width, 3-Hz repetition rate). Mass spectra were acquired in the positive linear mode with delayed extraction. The instrument's default mass calibration was used. The matrix used was 10 mg mL^{-1} sinapinic acid in a 1:1 solution of acetonitrile and 0.1% trifluoroacetic acid. The predicted molecular mass of each mutant protein was calculated using MS-digest of ProteinProspector (http://prospector.ucsf.edu).

Lipid-Binding Assay

LUVs at a concentration of 10 mg mL^{-1} in 40 mM Tris-HCl, pH 7.4, were prepared using an extrusion method described previously (Hope et al., 1985). The LUV suspensions were incubated with DHN1 proteins at a 15:1 mass ratio of phospholipid to protein for 3 h at 25°C, as described previously (Koag et al., 2003). To separate each protein in a free state from its liposome-associated form, the incubation mixtures were applied to a calibrated Superose 6 (10 mm × 30 cm) gel filtration column (Amersham Pharmacia) and eluted at a rate of 0.5 mL min^{-1} with 40 mM Tris-HCl (pH 7.4). The presence of DHN protein in each fraction was analyzed by immunoblotting, and the concentration of phospholipid was determined as described previously (Koag et al., 2003).

CD Spectrometry

The CD spectrum of each DHN1 protein in 20 mM sodium phosphate (pH 7.0) or in the presence of liposomes was measured over the range of 190 to 250 nm at 25°C in a 0.1-cm path length quartz cuvette using a Jasco J-715 spectropolarimeter (University of California, Irvine) as described previously (Koag et al., 2003). SUVs at the concentration of 1 mg mL^{-1} in 20 mM sodium phosphate (pH 7.0) were prepared using sonification and ultracentrifugation as described previously (Koag et al., 2003). The spectra were corrected against buffer and liposome. Similarly, the CD spectrum of each DHN1 protein or K-segment peptide in 50 mM NaCl (pH 7.0) or in the presence of 10 mM SDS and 50 mM NaCl was measured using a Jasco J-815 spectropolarimeter at the University of California, Riverside. These spectra were corrected against NaCl and SDS. In addition, the K-segment peptide was examined in 20 mM sodium phosphate (pH 7.0) with or without liposomes using a Jasco J-715 spectropolarimeter at the University of California, Irvine, with or without SDS using a Jasco J-815 spectropolarimeter at the University of California, Riverside. The mean residue ellipticity was presented as a function of wavelength. CD data from 190 to 250 nm were analyzed to estimate the secondary structure composition using the CDSSTR program in Dichroweb (http://dichroweb.cryst.bbk.ac.uk; Whitmore and Wallace, 2004).

Protein Concentration

The concentration of each purified protein was determined using a M_r and molar extinction coefficient of each protein at 280 nm, calculated on the basis of the amino acid sequence of each protein (Gill and von Hippel, 1989).

Amino Acid Analysis

The amino acid composition of each protein was determined to confirm the identity of each purified protein at the University of Nevada Protein Structure Core Facility using a 6-aminoquinoyl-*N*-hydroxylsuccinimidyl carbamate pre-column derivatization procedure (Cohen and Michaud, 1993). Hydrolysates of derivatized amino acids were separated on a reverse-phase AccQ Tag C18 column (Waters). The quantity of each amino acid was calculated using a standard curve obtained using Pierce Amino Acid Standard H. The amino acid composition of wild-type DHN was reported previously (Campbell et al., 1998).

Synthesis of the K-Segment Peptide

The DHN K-segment peptide (TGEKKGIMDKIKEKLPGQH; M_r = 2,022.43), synthesized using standard Fmoc solid-phase synthesis chemistry, was provided by Dr. Dallas Rabenstein and Peter Ladjimi (Department of Chemistry, University of California, Riverside).

Supplemental Data

The following materials are available in the online version of this article.

Supplemental Figure S1. Comparison of nucleotide and amino acid sequences of wild-type DHN1 and deletion mutants.

Supplemental Figure S2. SDS-PAGE of purified K-segment deletion proteins.

Supplemental Table S1. M_r and pI of wild type and each mutant protein.

Supplemental Table S2. Amino acid composition of wild type and each mutant protein.

ACKNOWLEDGMENTS

We thank Dr. Robert Richard (University of California, Riverside) and Dr. Kym F. Faull (University of California, Los Angeles) for advice on mass spectrometry and Dr. Stephan White (University of California, Irvine) for use of a the J-715 spectropolarimeter.

Received February 5, 2009; accepted May 6, 2009; published May 13, 2009.

LITERATURE CITED

Alsheikh MK, Heyen BJ, Randall SK (2003) Ion binding properties of the dehydrin ERD14 are dependent upon phosphorylation. J Biol Chem **278:** 40882–40889

Alsheikh MK, Svensson JT, Randall SK (2005) Phosphorylation regulated ion-binding is a property shared by the acidic subclass of dehydrins. Plant Cell Environ **28:** 1114–1122

Andersson MX, Kjellberg JM, Sandelius AS (2001) Chloroplast biogenesis: regulation of lipid transport to the thylakoid in chloroplasts isolated from expanding and fully expanded leaves of pea. Plant Physiol **127:** 184–193

Artus NN, Uemura M, Steponkus PL, Gilmore SJ, Lin C, Thomashow MF (1996) Constitutive expression of the cold-regulated *Arabidopsis thaliana COR15a* gene affects both chloroplast and protoplast freezing tolerance. Proc Natl Acad Sci USA **93:** 13404–13409

Asghar R, Fenton RD, DeMason DA, Close TJ (1994) Nuclear and cytoplasmic localization of maize embryo and aleurone dehydrin. Protoplasma **177:** 87–94

Bokor M, Csizmok V, Kovacs D, Banki P, Friedrich P, Tompa P, Tompa K (2005) NMR relaxation studies on the hydrate layer of intrinsically unstructured proteins. Biophys J **88:** 2030–2037

Brini F, Hanin M, Lumbreras V, Irar S, Pages M, Masmoudi K (2006) Functional characterization of DHN-5, a dehydrin showing a differential phosphorylation pattern in two Tunisian durum wheat (*Triticum durum* Desf.) varieties with marked difference in salt and drought tolerance. Plant Sci **172:** 20–28

Campbell SA, Crone DE, Ceccardi TL, Close TJ (1998) A ca. 40 kDa maize (*Zea mays* L.) embryo dehydrin is encoded by the *dhn*2 locus on chromosome 9. Plant Mol Biol **38:** 417–423

Choi DW, Zhu B, Close TJ (1999) The barley (*Hordeum vulgare* L.) dehydrin multigene family: sequences, allelic types, chromosome assignments, and expression characteristics of 11 *Dhn* genes of cv. Dicktoo. Theor Appl Genet **98:** 1234–1247

Close TJ (1996) Dehydrins: emergence of a biochemical role of a family of plant dehydration proteins. Physiol Plant **97:** 795–803

Close TJ (1997) Dehydrins: a commonality in the response of plants in dehydration and low temperature. Physiol Plant **100:** 291–296

Close TJ, Fenton RD, Moonan F (1993) A view of plant dehydrins using antibodies specific to the carboxy terminal peptide. Plant Mol Biol **23:** 279–286

Cohen SA, Michaud DP (1993) Synthesis of a fluorescent derivatizing reagent, 6-aminoquinolyl-N-hydroxysuccinimidyl carbamate, and its application for the analysis of hydrolysate amino acids via high-performance liquid chromatography. Anal Biochem **211:** 279–287

Cullis PR, Hope MJ, Tilcock CPS (1986) Lipid polymorphism and the roles of lipids in membranes. Chem Phys Lipids **40:** 127–144

Dalal K, Pio F (2006) Thermodynamics and stability of the PAAD/DAPIN/PYRIN domain of IFI-16. FEBS Lett **580:** 3083–3090

Danyluk J, Perron A, Houde M, Limin A, Fowler B, Benhamou N, Sarhan F (1998) Accumulation of an acidic dehydrin in the vicinity of the plasma membrane during cold acclimation of wheat. Plant Cell **10:** 623–638

Dure L III (1993) Structural motifs in LEA proteins of higher plants. *In* TJ Close, BA Bray, eds, Response of Plants to Cellular Dehydration during Environmental Stress. American Society of Plant Physiologists, Rockville, MD, pp 91–103

Dyson HJ, Wright PE (2005) Intrinsically unstructured proteins and their functions. Nat Rev Mol Cell Biol **6:** 197–208

Egerton-Warburton LM, Balsamo RA, Close TJ (1997) Temporal accumulation and ultrastructural localization of dehydrins in *Zea mays* L. Physiol Plant **101:** 545–555

Epand RM, Shai Y, Segrest JP, Anantharamaiah GM (1995) Mechanisms for the modulation of membrane bilayer properties by amphipathic helical peptides. Biopolymers **37:** 319–338

Fowler DB, Breton G, Limin AE, Mahfoozi S, Sarhan F (2001) Photoperiod and temperature interactions regulate low-temperature-induced gene expression in barley. Plant Physiol **127:** 1676–1681

Frank W, Munnik T, Kerkmann K, Salamini F, Bartels D (2000) Water deficit triggers phospholipase D activity in the resurrection plant *Craterostigma plantagineum*. Plant Cell **12:** 111–123

Garay-Arroyo A, Colmenero-Flores JM, Garciarrubio A, Covarrubias AA (2000) Highly hydrophilic proteins in prokaryotes and eukaryotes are common during conditions of water deficit. J Biol Chem **275:** 5668–5674

Gill SC, von Hippel PH (1989) Calculation of protein extinction coefficients from amino acid sequence data. Anal Biochem **182:** 319–326

Godoy JA, Lunar R, Torresschumann S, Moreno J, Rodrigo RM, Pintortoro JA (1994) Expression, tissue distribution and subcellular-localization of dehydrin Tas14 in salt-stressed tomato plants. Plant Mol Biol **26:** 1921–1934

Goyal K, Tisi L, Basran A, Browne J, Burnell A, Zurdo J, Tunnacliffe A (2003) Transition from natively unfolded to folded state induced by desiccation in an anhydrobiotic nematode protein. J Biol Chem **278:** 12977–12984

Hara M, Fujinaga M, Kuboi T (2005) Metal binding by citrus dehydrin with histidine-rich domains. J Exp Bot **56:** 2695–2703

Hara M, Tereashima S, Fukava T, Kuboi T (2003) Enhancement of cold tolerance and inhibition of lipid peroxidation by citrus dehydrin in transgenic tobacco. Planta **217:** 290–298

Heyen BJ, Alsheikh MK, Smith EA, Torvik KF, Seals DF, Randall SK (2002) The calcium-binding activity of a vacuole-associated, dehydrin-like protein is regulated by phosphorylation. Plant Physiol **130:** 675–687

Hillenkamp H, Karas M, Beavis RC, Chait BT (1991) Matrix-assisted laser desorption/ionization mass spectrometry of biopolymers. Anal Chem **63:** 1193–1203

Hope MJ, Bally MB, Webb G, Cullis PR (1985) Production of large unilamellar vesicles by a rapid extrusion procedure: characterization of size distribution, trapped volume and ability to maintain a membrane potential. Biochim Biophys Acta **812:** 55–65

Houde M, Daniel C, Lachapelle M, Allard F, Laliberté S, Sarhan F (1995) Immunolocalization of freezing-tolerance-associated proteins in the cytoplasm and nucleoplasm of wheat crown tissue. Plant J **8:** 583–593

Ingram J, Bartels D (1996) The molecular basis of dehydration tolerance in plants. Annu Rev Plant Physiol Plant Mol Biol **47:** 377–403

Ismail AM, Hall AE, Close TJ (1999a) Allelic variation of a dehydrin gene cosegregates with chilling tolerance during seedling emergence. Proc Natl Acad Sci USA **96:** 13566–13570

Ismail AM, Hall AE, Close TJ (1999b) Purification and partial characterization of a dehydrin involved in chilling tolerance during seedling emergence of cowpea. Plant Physiol **120:** 237–244

Jayaprakash TL, Ramamohan G, Krishnaprasad BT, Ganeshkumar, Prasad TG, Mathew MK, Udayakumar M (1998) Genotypic variability in differential expression of *lea*2 and *lea*3 genes and proteins in response to salinity stress in fingermillet (*Eleusine coracana* Gaertn) and rice (*Oryza sativa* L.) seedlings. Ann Bot (Lond) **82:** 513–522

Jensen AB, Goday A, Figueras M, Jessop AC, Pages M (1998) Phosphorylation mediates the nuclear targeting of the maize Rab17 protein. Plant J **13:** 691–697

Jepson SG, Close TJ (1995) Purification of a maize dehydrin protein expressed in *Escherichia coli*. Protein Expr Purif **6:** 632–636

Katagiri T, Ishiyama K, Kato T, Tabata S, Kobayashi M, Shinozaki K (2005) An important role of phosphatidic acid in ABA signaling during germination in *Arabidopsis thaliana*. Plant J **43:** 107–117

Kitchen J, Saunders RE, Warwicker J (2008) Charge environments around phosphorylation sites in proteins. BMC Struct Biol **8:** 19

Koag MC (2002) The binding of maize Dehydrin1 to anionic phospholipid vesicles and the role of K-segment in the lipid binding. PhD thesis. University of California, Riverside, CA

Koag MC, Fenton RD, Wilkens S, Close TJ (2003) The binding of maize DHN1 to lipid vesicles carrying anionic phospholipids is associated with increased α-helicity of the protein. Plant Physiol **131:** 309–316

Kovacs D, Kalmar E, Torok Z, Tompa P (2008) Chaperone activity of ERD10 and ERD14, two disordered stress-related plant proteins. Plant Physiol **147:** 381–390

Kruger C, Berkowitz O, Stephan UW, Hell R (2002) A metal-binding

member of the late embryogenesis abundant protein family transports iron in the phloem of *Ricinus communis* L. J Biol Chem **277:** 25062–25069

Liscovitch M, Cantley LC (1995) Signal transduction and membrane traffic: the PITP/phosphoinositide connection. Cell **81:** 659–662

Lisse T, Bartels D, Kalbitzer HR, Jaenicke R (1996) The recombinant dehydrin-like desiccation stress protein from the resurrection plant *Craterostigma plantagineum* displays no defined three-dimensional structure in its native state. Biol Chem **377:** 555–567

McCubbin WD, Kay CM, Lane BG (1985) Hydrodynamic and optical properties of the wheat germ E_m protein. Can J Biochem Cell Biol **63:** 803–811

Mishra VK, Palgunachari MN (1996) Interaction of model class A1, class A2, and class Y amphipathic helical peptides with membranes. Biochemistry **35:** 11210–11220

Mouillon JM, Eriksson SK, Harryson P (2008) Mimicking the plant cell interior under water stress by macromolecular crowding: disordered dehydrin proteins are highly resistant to structural collapse. Plant Physiol **148:** 1925–1937

Mouillon JM, Gustafsson P, Harryson P (2006) Structural investigation of disordered stress proteins: comparison of full-length dehydrins with isolated peptides of their conserved segments. Plant Physiol **141:** 638–650

Nylander M, Svensson J, Palva ET, Welin BV (2001) Stress-induced accumulation and tissue-specific localization of dehydrins in *Arabidopsis thaliana*. Plant Mol Biol **45:** 263–279

Oldfield CJ, Cheng Y, Cortese MS, Brown CJ, Uversky VN, Dunker AK (2005) Comparing and combining predictors of mostly disordered proteins. Biochemistry **44:** 1989–2000

Prestrelski SJ, Tedeschi N, Arakawa T, Carpenter JF (1993) Dehydration-induced conformational transitions in proteins and their inhibition by stabilizers. Biophys J **65:** 661–671

Prinz H, Lavie A, Scheidig AJ, Spangenberg O, Konrad M (1999) Binding of nucleotide to guanylate kinase, $p21^{ras}$, and nucleotide-diphosphate kinase studied by nano-electrospray mass spectrometry. J Biol Chem **274:** 35337–35342

Puhakainen T, Hess MW, Pirjo Makela P, Svensson J, Heino P, Palva ET (2004) Overexpression of multiple dehydrin genes enhances tolerance to freezing stress in Arabidopsis. Plant Mol Biol **54:** 743–753

Roberts JK, DeSimone NA, Lingle WL, Dure L (1993) Cellular concentrations and uniformity of cell type accumulation of two Lea proteins in cotton embryos. Plant Cell **5:** 769–780

Rodriguez EM, Svensson J, Malatrasi M, Choi DW, Close TJ (2005) Barley *Dhn*13 encodes a KS-type dehydrin with constitutive and stress responsive expression. Theor Appl Genet **110:** 852–858

Rorat T, Grygorowicz WJ, Irzykowski W, Rey P (2004) Expression of KS-type dehydrins is primarily regulated by factors related to organ type and leaf developmental stage during vegetative growth. Planta **218:** 878–885

Rorat T, Szabala BM, Grygorowicz WJ, Wojtowicz B, Yin Z, Rey P (2006) Expression of SK_3-type dehydrin in transporting organs is associated with cold acclimation in *Solanum* species. Planta **224:** 205–221

Shih MD, Lin SC, Hsieh JS, Tsou CH, Chow TY, Hsing YI (2004) Gene cloning and characterization of a soybean (*Glycine max* L.) LEA protein, GmPM16. Plant Mol Biol **56:** 689–703

Soulages JL, Kim K, Arrese EL, Walters C, Cushman JC (2003) Conformation of a group 2 late embryogenesis abundant protein from soybean: evidence of poly (L-proline)-type II structure. Plant Physiol **131:** 963–975

Steponkus PL, Uemera M, Joseph RA, Gilmour SJ, Thomashow MF (1998) Mode of action of the *COR15a* gene on the freezing tolerance of *Arabidopsis thaliana*. Proc Natl Acad Sci USA **95:** 14570–14575

Svensson J, Ismail A, Palva ET, Close TJ (2002) Dehydrins. *In* KB Storey and JB Storey eds, Cell and Molecular Responses to Stress. Elsevier Science, Amsterdam, The Netherlands, pp 155–171

Svensson J, Palva ET, Welin B (2000) Purification of recombinant Arabidopsis thaliana dehydrins by metal ion affinity chromatography. Protein Expr Purif **20:** 169–178

Tolleter D, Jaquinod M, Mangavel C, Passirani C, Saulnier P, Manon S, Teyssier E, Payet N, Avelange-Macherel MH, Macherel D (2007) Structure and function of a mitochondrial late embryogenesis abundant protein are revealed by desiccation. Plant Cell **19:** 1580–1589

Tommasini L, Svensson JT, Rodriguez EM, Wahlid A, Malatrasi M, Kato K, Wanamaker S, Resnik J, Close TJ (2008) Dehydrin gene expression provides an indicator of low temperature and drought stress: transcriptome-based analysis of barley (*Hordeum vulgare* L.). Funct Integr Genomics **8:** 387–405

Tompa P (2002) Intrinsically unstructured proteins. Trends Biochem Sci **27:** 527–533

Tompa P (2005) The interplay between structure and function in intrinsically unstructured proteins. FEBS Lett **579:** 3346–3354

Tompa P, Banki P, Bokor M, Kamasa P, Kovacs D, Lasanda G, Tompa K (2006) Protein-water and protein-buffer interactions in the aqueous solution of an intrinsically unstructured plant dehydrin: NMR intensity and DSC aspects. Biophys J **91:** 2243–2249

Uversky VN (2002) What does it mean to be natively unfolded? Eur J Biochem **269:** 2–12

White SH, Ladokhin AS, Jayasinghe S, Hristova K (2001) How membranes shape protein structure. J Biol Chem **276:** 32395–32398

Whitmore L, Wallace BA (2004) DICHROWEB, an online server for protein secondary structure analyses from circular dichroism spectroscopic data. Nucleic Acids Res **32:** W668–W673

Whitsitt MS, Collins RG, Mullet JE (1997) Modulation of dehydration tolerance in soybean seedlings. Plant Physiol **114:** 917–925

Wright PE, Dyson JH (1999) Intrinsically unstructured proteins: re-assessing the protein structure-function paradigm. J Mol Biol **293:** 321–331

Zhu B, Choi DW, Fenton R, Close TJ (2000) Expression of the barley dehydrin multigene family and the development of freezing tolerance. Mol Gen Genet **264:** 145–153